

# MILP-based Model Predictive Control of Electric Vehicle Fleet Charging in the presence of Electricity Production from Renewable Energy Sources

Luka Grden, Branimir Škugor and Joško Deur  
University of Zagreb, Zagreb, Croatia  
Faculty of Mechanical Engineering and Naval Architecture  
e-mail: luka.grden@fsb.unizg.hr, branimir.skugor@fsb.unizg.hr, josko.deur@fsb.unizg.hr

## ABSTRACT

Electric vehicles (EV) play a crucial role in transforming the transportation sector to become more sustainable, cleaner, and energy efficient. Given that EVs are generally parked and ready for charging for a great majority of time, advanced charging management techniques can take advantage of this opportunity to lower charging costs and more effectively harness the potential of renewable energy sources (RES). To address this objective, the paper proposes an optimal charging management strategy based on model predictive control (MPC), which relies on a mixed-integer linear programming (MILP) algorithm for online optimization of charging power of individual EVs within a fleet. The proposed strategy is formulated in two forms: (i) direct optimization of individual EV charging power and (ii) optimization of aggregate charging power distributed to individual EVs through a heuristic algorithm (hierarchical approach). The two strategies are evaluated against an offline optimization benchmark in terms of charging cost, RES energy utilization, and related optimization time execution for the case of one-week period, virtually electrified delivery vehicle fleet of a local retail company, and a two-tariff electricity price model. A dumb charging strategy, which simply performs charging under maximal power immediately upon EVs connection, is also used as an evaluation baseline.

## KEYWORDS

Electric vehicle fleet, optimal charging, mixed-integer linear programming, model predictive control, single-level charging, hierarchical charging, renewable energy sources

## INTRODUCTION

The last decade has seen a significant shift in the global automotive industry towards plug-in electric vehicles (EVs). However, despite distinctive benefits of EVs, such as reduced pollutant and greenhouse gas emissions and lower operating costs, with their growing adoption, there are challenges arising from the need for adequate electricity infrastructure supported and related smart charging management solutions. Proper charging management can lead to charging cost reduction [1], balanced daily load profile on the grid [2], and reduction of the overall system emissions by maximising renewable energy sources (RES) exploitation [3]. To this end, an offline charging optimization, executed usually over a longer period (e.g., weeks or months), is typically used for investigating the potential of conventional fleet electrification through techno-economic analyses [4]. Depending on the considered scenario and available data used, a range of optimization techniques are exploited in literature for this task, such as dynamic, mixed-integer, and quadratic programming algorithms [1, 5, 6], robust and stochastic optimization methods [7, 8], and genetic algorithms [9]. The results of offline optimizations are often utilised as benchmarks for validating online (real-time) charging management strategies. In the context of real-time charging, an appealing technique is model predictive control (MPC) (see a conceptual illustration in Figure 1), which is characterized by its ability to account for multiple constraints on state and control variables and different predictions over a time horizon

while performing optimization in each sampling time step. For instance, authors in [10] propose an event-driven MPC framework for EV charging, aiming to minimise cost of energy consumption by tracking of a reference load profile defined by a grid system operator. To include EV drivers' preferences, available charging time, and other technical constraints, the real-time optimization problem is formulated as a mixed-integer program (MILP) [10]. Similarly, an economic MPC charging strategy based on linear programming (LP) is used in [11], where full information about the electricity price time profile and State-of-Charge (SoC) of arriving EVs is assumed to be known. The results are also validated for the case of arriving EVs' SoC uncertainty, showing a minor impact on the final cost. Additional savings can be achieved by introducing electricity production from renewable energy sources (e.g., solar or wind energy), thus contributing to the overall efficiency and independence of the local grid [12]. In this regard, an EV fleet can be used as a distributed energy storage for the maximal utilization of RES production. In that way, a fleet connected to the grid, using advanced charging management, can actively participate in regulating the load of the power grid, as well as in electricity markets. An interesting robust MPC approach handling intermittent nature of RES and EV charging demand uncertainty, while also considering the limited space at charging station, is proposed and discussed in [13]. Here, the objective is to increase the profit margin by providing the charging service to a maximum number of EV drivers. Similarly, in [5], a system that utilizes a stationary battery energy storage system (BESS) along with EV batteries is managed, with the aim to store excessive RES energy in BESS and use it for EV charging in periods of high electricity price.

While the above-outlined real-time charging strategies optimize the charging power directly at the level of individual EVs (single-level charging), an alternative hierarchical approach is proposed in [14]. Here, the real-time optimization of charging power is performed on the aggregate level where the whole EV fleet is considered as a single aggregate battery, and the obtained optimal aggregate charging power is distributed over individual EVs using a rule-based algorithm. Similar approach is addressed in [15] for electric buses, where the goal is not only to reduce charging costs but also to mitigate the local grid overload. The quadratic-cost charging power optimization is performed in real-time, and the aggregated power is then distributed using a fuzzy logic, considering the charging urgency depending on departure time and current SoC. In general, when compared to a single-level charging, hierarchical charging strategies are characterised by improved computational efficiency and scalability for an increased number of vehicles (see, e.g., its application to a fleet of 1000 EVs on the level of whole city in [16]), while introducing certain suboptimality due to inherent errors of aggregate modelling approach.

This paper provides a single-level charging approach based on linear programming (LP) and mixed-integer linear programming (MILP) optimization techniques, used often for scheduling and planning purposes in general, as well as in the context of EV charging [5, 10, 11, 14, 16]. The MILP technique is applied due to the need to incorporate energy production from RES into the optimization problem, which introduces discontinuities and thus makes the LP formulation unsuitable. The proposed charging method is systematically verified against an offline optimization benchmark and a hierarchical dynamic programming (DP)-based charging approach proposed in the accompanying paper [17], for the scenario of virtually electrified delivery vehicle fleet of a local retail company and two-tariff electricity price model.

In summary, the main contributions of the paper are: (i) setting up a MILP-based MPC for a single-level EV fleet charging management accounting for production from RES, and (ii)

systematically evaluating the proposed method against the hierarchical method and the offline benchmark obtained by MILP.

The remaining part of the paper is organized as follows. Sections II and III describe EV fleet models and an offline charging management optimization, respectively, where the latter is aimed at setting the globally optimal benchmark. Section IV elaborates on real-time charging methods, while Section V presents simulation results. Finally, concluding remarks are given in Section VI.

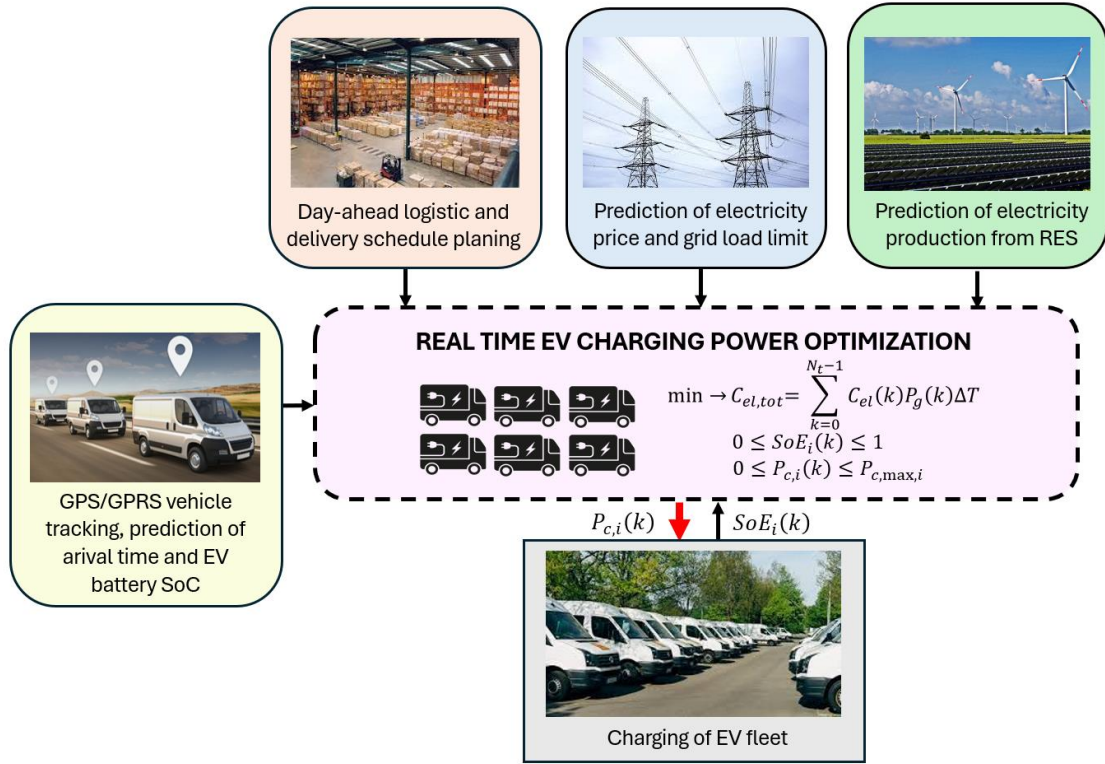


Figure 1. Conceptual illustration of optimization-based EV fleet charging management

## EV FLEET MODELS

This section presents EV fleet models used as a basis for charging optimization and simulations. The focus is on the distributed model where each EV is modelled separately, while more details on the EV fleet aggregate modelling approach are given in the accompanying paper [17].

### Distributed EV fleet model for charging power optimization

The EV batteries are modelled as energy storages with the state of energy  $SoE_i$  as a state variable and the charging power  $P_{c,i}$  as a control variable. A discrete-time state equation of the individual  $i^{\text{th}}$  battery, can be written as follows:

$$SoE_i(k+1) = SoE_i(k) + SoE_{in,i}(k)n_{in,i}(k) - SoE_{out,i}(k)n_{out,i}(k) + \eta_{ch} \frac{P_{c,i}(k)\Delta T}{E_{c,max,i}}, \quad k = 0, 1, \dots, N_t - 1, \quad (1)$$

where the index  $i$  denotes the specific EV within the fleet ( $i = 0, 1, \dots, N_v$ ), with  $N_v$  denoting the total number of EVs in the fleet. The variable  $k$  marks the discrete time step,  $N_t$  is the total number of those steps,  $SoE_{in,i}$  and  $SoE_{out,i}$  are the energy levels of individual EVs that connect and disconnect from the grid within the  $k^{\text{th}}$  step, respectively, and  $n_{in,i}$  and  $n_{out,i}$  represent binary

variables taking values of one or zero for grid connection or disconnection, respectively. The parameter  $E_{c,max,i}$  is the maximum energy capacity of  $i^{\text{th}}$  EV battery,  $\eta_{ch}$  is the charging efficiency, and  $\Delta T$  is the discretisation time step (here set to  $\Delta T = 0.25$  h which corresponds to 15 min). The state variable SoE is defined as  $SoE_i = E_{c,i}/E_{c,max,i}$ , where  $E_{c,i}$  is the battery energy of  $i^{\text{th}}$  EV, which equals the actual battery energy if EV is connected within the  $k^{\text{th}}$  time step, while it is zero otherwise. The state variable is limited in the range from zero to one:

$$0 \leq SoE_i(k) \leq n_{cb,i}(k), \quad n_{cb,i} \in \{0, 1\}, \quad (2)$$

where  $n_{cb,i}$  represents a binary variable indicating whether the vehicle is connected (partially or fully) to the charger within  $k^{\text{th}}$  step ( $n_{cb,i} = 1$ ) or not connected at all ( $n_{cb,i} = 0$ ). The battery charging power is limited only to positive values (i.e., one-directional power flow from the grid to EV is assumed), with the upper limit set to depend on the maximum charging power  $P_{c,max,i}$ :

$$0 \leq P_{c,i}(k) \leq n_{cs,i}(k)P_{c,max,i}, \quad n_{cs,i} \in [0, 1], \quad (3)$$

where  $n_{cs,i}$  expresses the share of time during which the EV is connected to the charger in the  $k^{\text{th}}$  step. Additionally, the aggregate charging power of the fleet is constrained by its upper limit:

$$\sum_{i=1}^{N_v} P_{c,i}(k) \leq P_{c,agg,max}. \quad (4)$$

where  $P_{c,agg,max}$  denotes the maximal power that could be drawn from the grid.

### Aggregate EV fleet model for charging power optimization

As opposed to the distributed EV fleet battery model, the aggregate model considers all EVs from the fleet as a single large battery, characterized by one state (SoE) and one control (charging power) variable (see [17] and [18] for more details). This approach relieves computational requirements but introduces certain inaccuracies in describing the fleet's behaviour due to aggregation effects and inability to capture nuances of individual vehicle interactions.

### Distributed EV fleet model for simulation study

To make the above distributed EV fleet model suitable for overall transport-energy system simulation purposes and satisfy all the required constraints, the state equation (1) is modified as follows [17]:

$$SoE_i(k) = \begin{cases} SoE_{int,i}(k), & \text{for } n_{out,i}(k) = 0, \\ 0, & \text{for } n_{out,i}(k) = 1. \end{cases} \quad (5)$$

In the case when the vehicle is connected to grid at the  $k^{\text{th}}$  step, the state variable  $SoE_i(k)$  assumes an intermediate value  $SoE_{int,i}$ , while it equals zero, otherwise. The intermediate value  $SoE_{int,i}$  consists of SoE increase contributions brought by the charging power  $P_{c,i}$  and EV connection to the grid ( $n_{in,i}(k) = 1$ ):

$$SoE_{int,i}(k) = SoE_i(k) + SoE_{in,i}(k)n_{in,i}(k) + \eta_{ch} \frac{P_{c,i}(k)\Delta T}{E_{c,max,i}}. \quad (6)$$

When the EV disconnects from the charger and a new driving mission starts (i.e.,  $n_{out,i}(k) = 1$ ), the variable  $SoE_{out,i}$  in  $(k+1)^{\text{th}}$  step takes on the value of  $SoE_{int,i}(k)$ :

$$SoE_{out,i}(k+1) = \begin{cases} SoE_{out,i}(k), & \text{for } n_{out,i}(k) = 0, \\ SoE_{int,i}(k), & \text{for } n_{out,i}(k) = 1. \end{cases} \quad (7)$$

On the other hand, in the case when the EV arrives from a driving mission and connects to the grid (i.e.,  $n_{in,i}(k) = 1$ ), the incoming state  $SoE_{in,i}$  is calculated by using a consumption function  $f_{SoC}$  whose value depends on the outgoing state  $SoE_{out,i}(k)$  and the distance of the related  $i^{\text{th}}$  driving mission  $d_i(k)$ :

$$SoE_{in,i}(k+1) = \begin{cases} 0, & \text{for } n_{in,i}(k) = 0, \\ f_{SoC}(SoE_{out,i}(k), d_i(k)), & \text{for } n_{in,i}(k) = 1. \end{cases} \quad (8)$$

The model (5)-(8) is accompanied by the individual charger power limit:

$$P_{c,max,i}(k) = \min \left( n_{cs,i}(k) P_{c,max,i}, \frac{1 - SoE_i(k) - SoE_{in,i}(k) n_{in,i}(k)}{\eta_{ch} \Delta T} E_{c,max,i} \right), \quad (9)$$

where the first term within the  $\min(\cdot)$  function refers to the upper charging power limit from Eq. (3), while the second one corresponds to the upper SoE limit derived from Eq. (6) for the case of  $SoE_{int,i} = 1$  (i.e., to prevent violation of SoE-related constraint (2)).

To encompass the aspect of maximum RES energy exploitation, the following condition is used:

$$P_g(k) = \begin{cases} -P_{res}(k) + \sum_{i=1}^{N_v} P_{c,i}(k), & \text{for } -P_{res}(k) + \sum_{i=1}^{N_v} P_{c,i}(k) \geq 0, \\ 0, & \text{for } -P_{res}(k) + \sum_{i=1}^{N_v} P_{c,i}(k) < 0, \end{cases} \quad (10)$$

where  $P_g$  refers to the power drawn from the grid,  $\sum_{i=1}^{N_v} P_{c,i}(k)$  is an aggregate EV fleet charging power request, and  $P_{res}$  is the power generated by RES. Namely, if the EV fleet charging power request is larger than the current RES production (the first condition in Eq. (10)), the RES power will be completely exploited and the remained power will be covered from the grid. Otherwise, i.e., if the fleet charging power request can be completely covered by the RES production (the second condition in Eq. (10)), the power drawn from the grid is zero.

## OFFLINE OPTIMIZATION OF EV FLEET CHARGING

The main goal of EV fleet charging optimization is to minimize the charging energy cost, while satisfying all the imposed constraints, given the assumed electricity price and RES production time profiles. The cost is defined as:

$$J = \sum_{k=0}^{N_t-1} C_{el}(k) P_g(k) \Delta T, \quad (11)$$

where  $C_{el}(k)$  is the time-varying electricity price (given in EUR/kWh), and the term  $P_g(k) \Delta T$  (expressed in kWh) represents the grid-supplied charging energy in the  $k^{\text{th}}$  step (see Eq. (10)). In the absence of RES energy production, the electricity drawn from the grid is equal to the total charging power given by  $P_g(k) = \sum_{i=1}^{N_v} P_{c,i}(k)$ , while otherwise the expression (10) applies. From the perspective of optimization, it should be emphasized that the individual charging power profiles  $P_{c,i}(k)$  represent the control variables to be optimized. The optimization problem is subject to the dynamic discrete-time fleet model Eq. (1) and inequality constraints given by Eqs. (2)-(4). Additionally, to satisfy the charge sustaining condition, i.e., to ensure that the SoE at end of optimization horizon,  $SoE_{final} = SoE_i(N_t)$ , is equal to the

initial one,  $SoE_{init} = SoE_i(0)$ , the following equality constraint is added to the optimization problem:

$$SoE_{final} = SoE_{init}. \quad (12)$$

### No RES included - LP formulation

In the case of no local RES, the above optimization problem is linear both in the cost function and constraints and can be represented in the general LP form [23]:

$$\min_{\mathbf{x}} \mathbf{c}^T \mathbf{x}, \quad (13a)$$

$$\text{s. t. } \mathbf{A}\mathbf{x} \leq \mathbf{b}, \quad \mathbf{x} \in \mathbb{R}^{n_x}, \quad (13b)$$

where  $\mathbf{c}^T$  is a cost vector and  $\mathbf{x}$  is an optimization vector to be determined to minimize the total cost  $\mathbf{c}^T \mathbf{x}$ , while satisfying linear inequality constraints contained within the matrix expression  $\mathbf{A}\mathbf{x} \leq \mathbf{b}$ . Considering the cost function (11), the vectors  $\mathbf{c}^T$  and  $\mathbf{x}$  can be defined as:

$$\mathbf{c}^T = [C_{el}(0) C_{el}(1) \dots C_{el}(N_t - 1)]\Delta T, \quad (14)$$

$$\mathbf{x} = [P_g(0) P_g(1) \dots P_g(N_t - 1)]^T. \quad (15)$$

The optimal control vector to be obtained for each EV within the fleet can be defined as:

$$\mathbf{u}_i = [P_{c,i}(0) P_{c,i}(1) \dots P_{c,i}(N_t - 1)]^T, \quad (16)$$

and similarly, the optimal state variables can be denoted as:

$$\mathbf{y}_i = [SoE_i(0) SoE_i(1) \dots SoE_i(N_t)]^T. \quad (17)$$

To comply with the state equation (1), the following equality constraint is set:

$$y_i(k+1) = y_i(k) + F_i(u_i(k)). \quad (18)$$

where  $F_i(u_i(k))$  reads (cf. Eq. (1)):

$$F_i(u_i(k)) = SoE_{in,i}(k)n_{in,i}(k) - SoE_{out,i}(k)n_{out,i}(k) + \eta_{ch} \frac{u_i(k)\Delta T}{E_{c,max,i}}. \quad (19)$$

In summary, the optimal LP charging problem, for  $i = 0, 1, \dots, N_v$ , and  $k = 0, 1, \dots, N_t - 1$ , can be written as:

$$\min_{\mathbf{u}_1, \mathbf{u}_2, \dots, \mathbf{u}_{N_v}} \mathbf{c}^T \mathbf{x}(\mathbf{u}_1, \mathbf{u}_2, \dots, \mathbf{u}_{N_v}) \quad (20a)$$

$$\text{s. t. } y_i(k+1) = y_i(k) + F_i(u_i(k)) \quad (20b)$$

$$y_i(0) = SoE_{init}, \quad (20c)$$

$$y_i(N_t) = SoE_{final}, \quad (20d)$$

$$\mathbf{0} \leq \mathbf{y}_i \leq \mathbf{n}_{cb,i} \quad (20e)$$

$$\mathbf{0} \leq \mathbf{u}_i \leq \mathbf{n}_{cs,i} P_{c,max,i}, \quad (20f)$$

$$\mathbf{0} \leq \mathbf{x} \leq \mathbf{P}_{c,agg,max}, \quad (20g)$$

where the constraints (20c) and (20d) define boundary SoE conditions (see Eq. (12)), while (20e), (20f), and (20g) relate to Eq. (2), Eq. (3), and Eq. (4), respectively.

### RES included - MILP formulation

In the case of including RES production in the optimal control problem formulation, the discontinuity in the form of conditional expression from Eq. (10) prevents the optimization from being solved with the standard LP method (13). To incorporate such discontinuity, a MILP formulation is employed, which includes additional optimization variables denoted as  $\mathbf{z}$ , limited only to integer values, i.e.  $\mathbf{z} \in \mathbb{Z}^{n_z}$ . Those variables are included in the problem via so called Big-M notation [19] (see Appendix for an example of transforming logical relations to inequality constraints appropriate for related solvers). In this regard, the optimal problem defined by Eq. (20) is expanded with integer optimization variables and logical relations as:

$$\min_{\mathbf{u}_1, \mathbf{u}_2, \dots, \mathbf{u}_{N_v}} \mathbf{c}^T \mathbf{x}(\mathbf{u}_1, \mathbf{u}_2, \dots, \mathbf{u}_{N_v}, \mathbf{z}), \quad (21a)$$

$$\text{s. t. Eqs. (20b) – (20g),} \quad (21b)$$

$$[z(k) = 1] \rightarrow P_g(k) = -P_{res}(k) + \sum_{i=1}^{N_v} u_i(k), \quad (21c)$$

$$[z(k) = 0] \rightarrow P_g(k) = 0, \quad (21d)$$

where  $\mathbf{z} = [z(0) z(1) \dots z(N_t - 1)]^T$  and  $z(k)$  in  $k^{\text{th}}$  step implies the cases for the grid power  $P_g(k)$  as specified in Eq. (10):

$$z(k) = \begin{cases} 1, & \text{for } -P_{res}(k) + \sum_{i=1}^{N_v} u_i(k) \geq 0, \\ 0, & \text{for } -P_{res}(k) + \sum_{i=1}^{N_v} u_i(k) < 0. \end{cases} \quad (22)$$

The LP and MILP formulations (20) and (21), respectively, are implemented within Matlab environment by using YALMIP optimization toolbox [20], and *linprog* and *intlinprog* solvers are used to solve the respective optimization problems.

### EV FLEET CHARGING MANAGEMENT

This section describes employment of LP- and MILP-based optimizations within the MPC framework for the real-time EV fleet charging.

#### Single-level charging

Unlike the offline optimization presented in the previous Section, where the calculation of optimal charging power is performed once over the entire time horizon considered (e.g., one week or one month), the MPC performs optimization in real-time (online) over a shorter receding horizon, i.e., at each discrete time step over a fixed-length prediction horizon window. In this study, the prediction horizon length  $N_p$  is set to 96 steps, corresponding to the period of one day (for  $\Delta T = 0.25$  h). To perform the MPC optimization, the input time profiles:  $n_{in,i}(j|k)$ ,  $n_{out,i}(j|k)$ ,  $SoE_{in,i}(j|k)$ ,  $SoE_{out,i}(j|k)$ ,  $C_{el}(j|k)$ ,  $P_{res}(j|k)$ ,  $n_{cb,i}(j|k)$ ,  $n_{cs,i}(j|k)$ , should be predicted in each sampling time step for the prediction horizon  $j = \{0, 1, \dots, N_p - 1\}$  relative to the current  $k^{\text{th}}$  step [17].

The real-time MPC optimization problem is formulated as follows in the case no RES:

$$\min_{\mathbf{u}_1, \mathbf{u}_2, \dots, \mathbf{u}_{N_v}} \sum_{j=0}^{N_p-1} \left( C_{ei}(j|k) P_g(j|k) \Delta T + K_s \sum_{i=1}^{N_v} SoE_{out,sl,i}(j|k) \right) \quad (23a)$$

$$\text{s. t. } y_i(j+1|k) = y_i(j|k) + F_i(u_i(j|k)), \forall i \in \{1, \dots, N_v\} \quad (23b)$$

$$y_i(0|k) = SoE_i(k), \quad (23c)$$

$$y_i(N_t|k) = SoE_{final}, \quad (23d)$$

$$0 \leq \mathbf{y}_i \leq \mathbf{n}_{cb,i}, \quad (23e)$$

$$0 \leq \mathbf{u}_i \leq \mathbf{n}_{cs,i} P_{c,max,i}, \quad (23f)$$

$$0 \leq \mathbf{P}_g \leq \mathbf{P}_{c,agg,max}, \quad (23g)$$

$$0 \leq \mathbf{SoE}_{out,sl,i}. \quad (23h)$$

Since the MPC controller is executed repetitively over time, the initial SoE of the optimization problem is equalized with the current  $SoE_i(k)$ , as denoted in Eq. (23c). For the results to be comparable with the offline optimization, an equality constraint has been added on the final state, Eq. (23d), only in the case when the end of prediction horizon reaches the end of simulation time (i.e.,  $k + N_p \geq N_t$ ). The remaining expressions (23e)-(23g) are set in the same way as in the case of offline optimization (cf. Eq. (20)). Additionally, to avoid feasibility problems, a slack variable  $SoE_{out,sl,i}(j|k)$  required to be positive via the constraint (23h) is introduced in Eq. (19) to read:

$$F_i(u_i(j|k)) = SoE_{in,i}(j|k) n_{in,i}(j|k) - \left( SoE_{out,i}(j|k) - SoE_{out,sl,i}(j|k) \right) n_{out,i}(k) + \eta_{ch} \frac{u_i(j|k) \Delta T}{E_{c,max,i}} \quad (24)$$

This is to account for the possibility that EV can sometimes leave the grid with SoE lower than that prescribed by  $SoE_{out,i}(j|k)$ , which can arise due to the charging power limitation given by Eq. (23f). To minimise this effect, the slack variable is penalised in the objective function (23a) with a penalization factor  $K_s$  set to a relatively high value of  $10^6$ .

Similarly, as in the case of offline optimization, the MPC problem formulation from Eq. (23) can be extended to include the energy production from RES (cf. Eqs. (21c)-(21d)) as:

$$[z(j|k) = 1] \rightarrow P_g(j|k) = -P_{res}(j|k) + \sum_{i=1}^{N_v} u_i(j|k), \quad (25a)$$

$$[z(j|k) = 0] \rightarrow P_g(j|k) = 0, \quad (25b)$$

with  $z(j|k)$  determined as in Eq. (22). The MPC optimization yields the optimal charging power sequences for each EV, and only the first values of those sequences  $u_i(0|k)$ ,  $i \in \{1, 2, \dots, N_v\}$ , are applied as the actual EV charging power (i.e., applied to the simulation model (5)-(9)), while all other values are discarded. The procedure is repeated in the upcoming sampling time steps.

### Hierarchical charging

To give a broader set of results, a hierarchical MPC charging strategy presented in the accompanying paper [17] is employed herein and it is outlined in what follows. In each sampling time step, the strategy performs charging power optimization on the aggregate level using the aggregate battery model and then distributes the obtained aggregate charging power to connected individual EVs using a heuristic/rule-based method. While the optimization on the



aggregate level is conducted by DP algorithm in [17], it is performed here by using LP/MILP formulation to be aligned with the proposed single-level charging strategies.

### Baseline (dumb) charging

Along with the above optimization-based charging strategies, additional so-called dumb charging is also considered to serve as a verification baseline. It simply performs charging at the maximal power available, starting from the moment of EV connection to the grid until reaching the maximal SoE or EV disconnection from the charger [17].

## RESULTS

### Case study and EV fleet model parameterization

The EV fleet models previously described are parameterised based on experimental GPS data recorded on 10 conventional mid-size delivery trucks of a local retail company (see details on the model parameterization in [17]). A battery energy consumption model  $f_{SoC}(\cdot)$  from Eq. (8), is obtained by simulations of extended range electric vehicle (EREV) model. The recorded GPS data provides information on EV availability for charging (Figure 2), which is assumed to take place in the distribution centre (DC). Note that vehicles activity pattern is rather repetitive over working days, i.e., with the highest activity around 10 a.m. (with the minimum number of vehicles at DC) and lowest during early morning around 5 a.m., when all vehicles are parked at DC. Figure 3a shows hypothetical electricity production from photovoltaic panels adopted from [4], while Figure 3b depicts the two-tariff electricity price model, both given over the considered one week period.

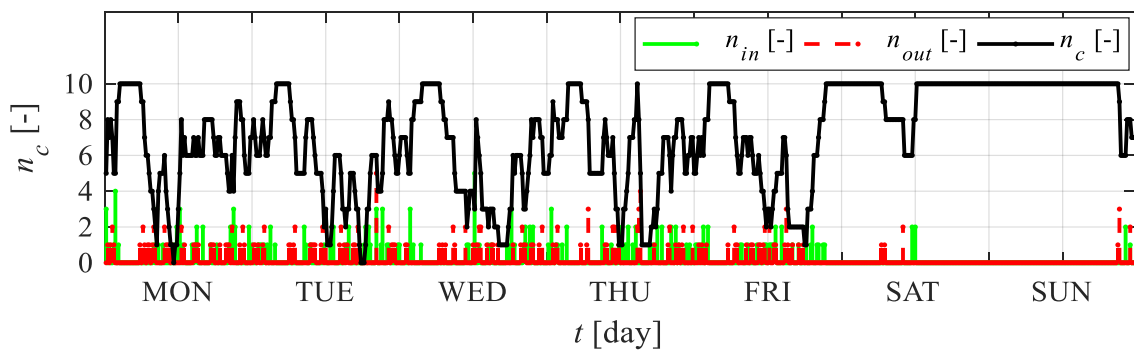
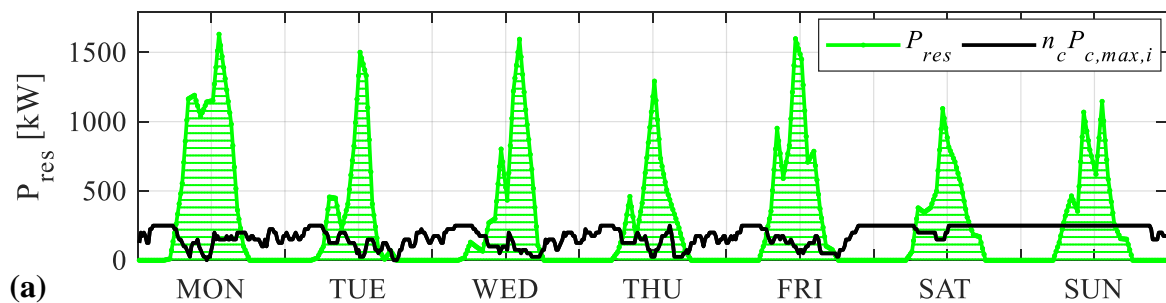


Figure 2. Time distributions of the number of EVs available for charging at DC ( $n_c$ ) and the distribution of vehicles arriving ( $n_{in}$ ) and departing ( $n_{out}$ ) from DC over a one week period



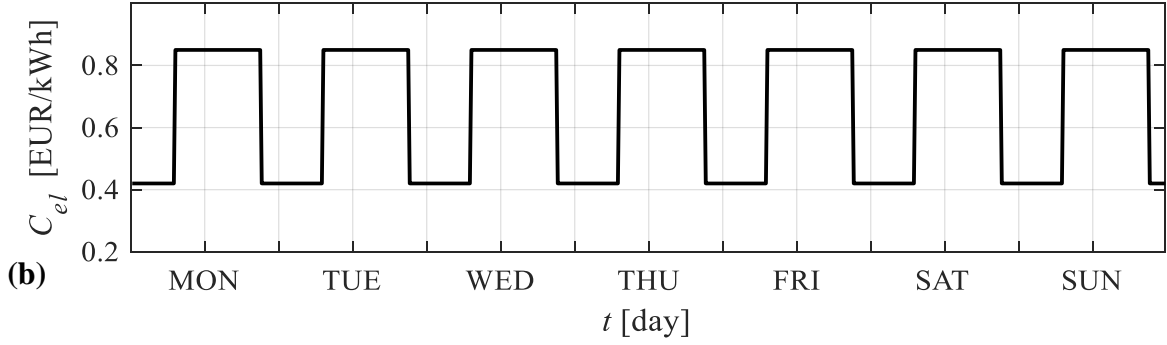


Figure 3. Hypothetical time profiles of RES energy production (a), and two-tariff electricity price profile (b)

From the above presented data, the following time profiles of EV fleet models are derived:  $n_{in,i}$ ,  $n_{out,i}$ ,  $n_{cb,i}$ ,  $n_{cs,i}$ , where  $i = 1, 2, \dots, N_v$ . The remaining parameters are set to:  $N_p = 96$ ,  $N_v = 10$ ,  $E_{c,max,i} = 72.67$  kWh,  $\eta_{ch} = 0.92$ ,  $SoE_{init} = 0.95$ ,  $SoE_{final} = 0.95$ ,  $P_{c,max,i} = 25$  kW,  $P_{c,agg,max} = 150$  kW,  $N_t = 672$ ,  $\Delta T = 0.25$  h [17].

### Results for case of no RES included

In Figure 4, the aggregate SoE and aggregate charging power time profiles (obtained from time profiles of individual EVs) are shown for different charging approaches. As expected, the baseline (DUMB) charging brings the SoE value very close to the upper limit ( $n_c/N_v$ ), because the vehicles are charged as soon as they arrive in DC. In the case of the globally optimal benchmark, OFF-LP, it is evident that most of the charging activity is shifted towards night hours, which is due to the cheaper electricity overnight (see Figure 3b). The MPC strategies exhibit similar charging power profiles to minimize related costs. Numerical values of the total fuel and energy consumption, and the charging costs are given in Table 1. Note that all strategies in Figure 4 end up around the same final target SoE value of 0.95 which facilitates fair comparison over related costs. To account for their minor differences, the specific cost

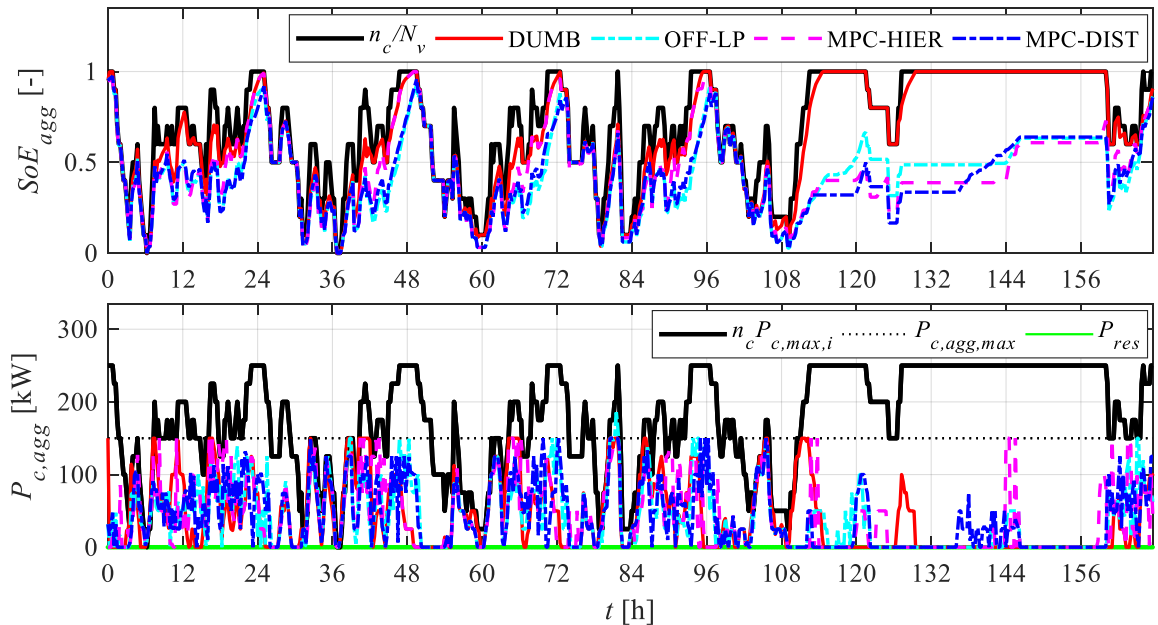


Figure 4. Aggregate SoE and charging power profiles obtained by different charging approaches applied to distributive battery model, with no RES considered

$C_{el,tot}/E_{c,tot}$  is also provided in the table. Firstly, the dumb charging results in around 10% higher cost with respect to the globally optimal benchmark OFF-LP, while this cost excess value equals 2.5% in the case of online hierarchical MPC (MPC-HIER). The increased cost of MPC-HIER may be attributed to the inaccuracies of the aggregate fleet optimization model and suboptimality of the heuristic aggregate charging power distribution method. On the other hand, the single-level MPC (MPC-DIST) approaches the benchmark within the margin of only 0.1%, and it is even slightly better in terms of specific cost, which is, however, at the cost of slightly higher fuel consumption.

Table 1. Comparison of different optimization approaches - no RES case

Charging profile	<sup>1</sup> $V_{fuel,tot}$ [l]	<sup>2</sup> $E_{c,tot}$ [kWh]	<sup>3</sup> $C_{el,tot}$ [EUR]	<sup>4</sup> $C_{el,tot}/E_{c,tot}$ [EUR/kWh]
DUMB	4273,4 (+0.3%)	6894.0 (+0.1%)	605.1 (+10.3%)	0.0878 (+10.2%)
OFF-LP	4259.8 (0.0%)	6885.2 (0.0%)	548.5 (0.0%)	0.0797 (0.0%)
MPC-HIER	4264.2 (+0.1%)	6872.7 (-0.2%)	561.8 (+2.4%)	0.0817 (+2.5%)
MPC-DIST	4263.0 (+0.07%)	6910.2 (+0.4%)	549.2 (+0.1%)	0.0795 (-0.3%)

<sup>1</sup>Total fuel consumption, <sup>2</sup>total charging energy, <sup>3</sup>total charging cost, <sup>4</sup>specific charging cost.

### Results for case of RES included

As shown in Figure 5, the introduction of RES leads to a more balanced charging power response throughout the week (OFF-MILP profiles; cf. Fig. 4), i.e., the charging activity is no longer solely concentrated over the low-electricity price intervals in the night, but also occurs

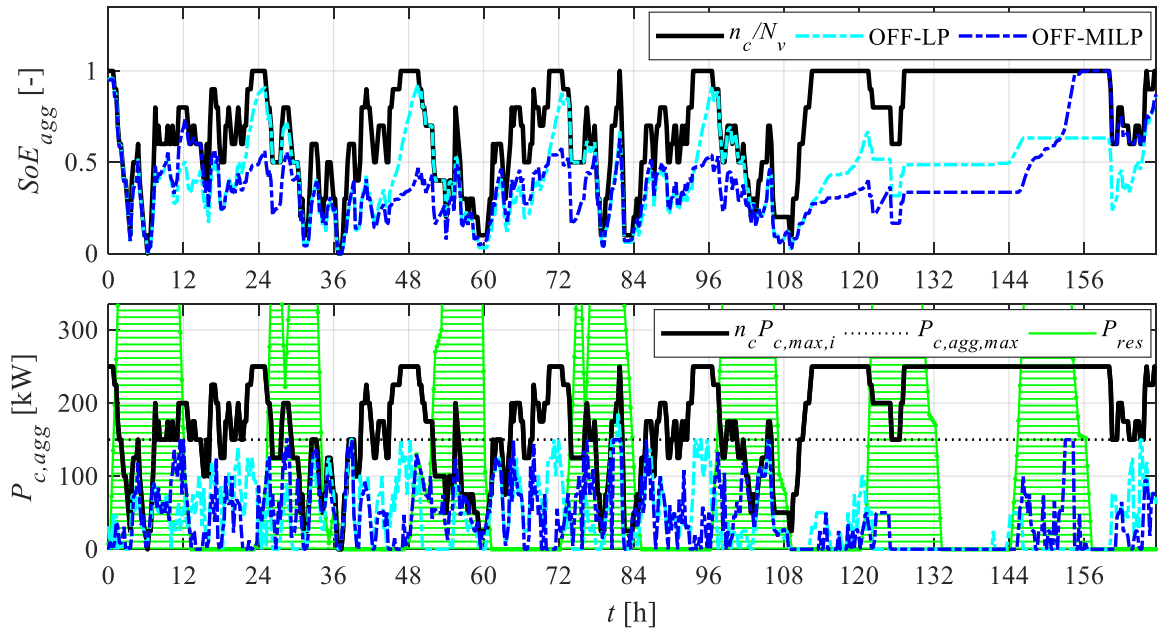


Figure 5. Comparative offline optimization results with RES included (OFF-MILP) and without RES (OFF-LP)

frequently at midday around solar noon, when the peak power generation by photovoltaic panels occurs (see green profiles).

Comparative results for the case of RES production included are given in Table 2. The charging cost of DUMB is now 86% higher than that of the benchmark OFF-MILP, which is substantially more pronounced than in the case of no RES considered (cf. Table 1). This can be attributed to relatively low RES energy utilization, where DUMB charging uses 44.3% less RES energy than OFF-MILP (see Figure 6). On the other hand, the difference between MPC results is now smaller than in the no RES case, with the specific total cost of MPC-HIER being only 0.8% higher than that of MPC-DIST and OFF-MILP. The RES energy utilization is relatively high both for MPC-HIER and MPC-DIST, being around 0.66 and comparable to that of OFF-MILP.

Table 2. Results of different charging approaches for one-week period and RES considered

Charging profile	<sup>1</sup> $V_{fuel,tot}$ [L]	<sup>2</sup> $E_{c,tot}$ [kWh]	<sup>3</sup> $E_{c,res}/E_{c,tot}$	<sup>4</sup> $C_{el,tot}$ [EUR]	<sup>5</sup> $C_{el,tot}/E_{c,tot}$ [EUR/kWh]
DUMB	4273,4 (+0.3%)	6894.0 (+0.1%)	0.3683 (-44.3%)	323.2 (+86.1%)	0.0466 (+77.0%)
OFF-MILP	4259.8 (0.0%)	6885.2 (0.0%)	0.6619 (0.0%)	173.7 (0.0%)	0.0252 (0.0%)
MPC-HIER	4262.9 (+0.1%)	6924.0 (+0.6%)	0.6585 (-0.5%)	176.1 (+1.4%)	0.0254 (+0.8%)
MPC-DIST	4263.0 (+0.1%)	6888.0 (+0.2%)	0.6783 (+2.5%)	173.9 (+0.1%)	0.0252 (0.0%)

<sup>1</sup>Total fuel consumption, <sup>2</sup>total charging energy, <sup>3</sup>utilization of RES energy, <sup>4</sup>total charging cost, <sup>5</sup>specific charging cost

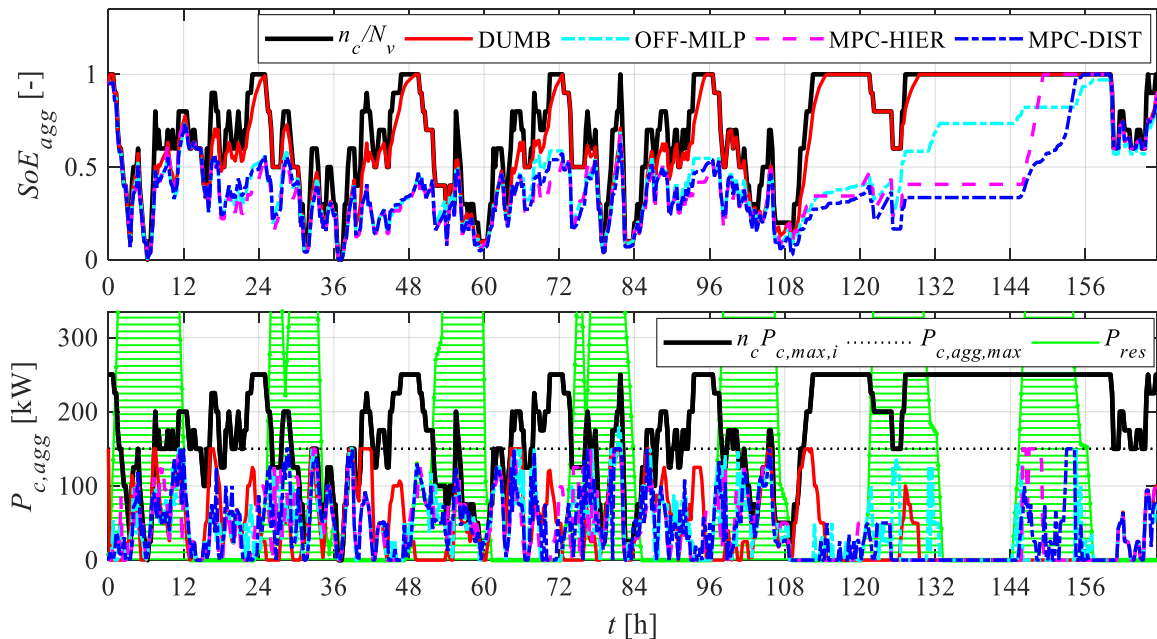


Figure 6. Aggregate SoE and charging power profiles obtained by different charging approaches applied to distributive battery model, with RES considered

In addition, when comparing the performance of control strategies, an important practical aspect is the optimization execution time, whose values are listed in Table 3 (executed on a computer with Intel(R) Core(TM) i5-8300H CPU @ 2.30GHz with 8 GB RAM installed). The optimal problem preparation time within YALMIP is included as well, as the initial creation of the parametric optimization model is a complex and time-consuming task. For the one-week horizon it takes 2.3 hours for the model preparation, and the optimization problem is then solved in 0.97 seconds when RES is not considered, and in 25.4 seconds when it is considered. The preparation time of 2.3 hours may seem long, but it is performed offline and only once and it, thus, does not represent an obstacle for application. The results demonstrate that the MPC-HIER strategy has by two orders of magnitude lower optimization execution time than the MPC-DIST strategy if RES is considered. The MPC-DIST optimization problem takes 24.8 seconds on average to execute, leading to a one-week scenario simulation lasting 4.6 hours. However, 24.8 seconds is still significantly lower than the time discretization of 15 minutes, meaning that it is satisfying for a real-time application for the given EV fleet size.

*Table 3. Comparison of execution times for optimizations with and without RES considered*

Charging profile	Optimal problem preparation time [s]	Solving one optimization problem [s]	Simulation time over one-week period [s]
No RES considered			
OFF-LP	8332.43 (2.3 hours)	0.97	-
MPC-HIER	5.43	0.02	13.10
MPC-DIST	37.12	0.05	26.41
RES considered			
OFF-MILP	8332.43 (2.3 hours)	25.40	-
MPC-HIER	1.18	0.71	477.12 (8 minutes)
MPC-DIST	30.33	24.77	16643.23 (4.6 hours)

## CONCLUSION

This paper has explored solutions for real-time electric vehicle (EV) fleet charging management, aiming to minimize charging costs and maximize exploitation of renewable energy sources (RES). The optimization performed offline over the full-time horizon was taken as the globally optimal benchmark, to assess the proposed real-time model predictive control (MPC) charging strategies. The proposed so-called single-level optimization was formulated in the form of linear programming (LP) in the case of no RES production, or in the form of mixed integer linear programming (MILP) in the case of RES production, to directly optimize charging power of each individual EV within the fleet. It was compared against an alternative hierarchical approach, performing the charging optimization on the aggregate level and distributing the obtained aggregate charging power over individual EVs through a heuristic method. A simple so-called dumb charging method performing charging with the maximum power immediately upon EV connection was additionally utilized to serve as a baseline for assessment of the other, more advanced methods.

The proposed strategies have been demonstrated for the scenario of virtually electrified conventional delivery vehicle fleet, whose charging schedules and power demand time profiles

were derived from experimental data and EV model simulations. In the absence of RES, the dumb charging results in around 10% higher charging cost compared to the offline LP benchmark. The hierarchical MPC approaches the offline benchmark within a margin of 2.4%, while this margin equals only 0.1% for the main, single-level MPC. In the case of RES production included, the dumb charging results in 86% higher charging cost compared to the offline MILP benchmark, while this cost excess equals only 1.4% in the case of hierarchical strategy. The proposed single-level charging is almost equivalent to the global optimum. In terms of related optimization execution time, the hierarchical method yields superior performance with respect to single-level approach (two orders of magnitude faster when RES production is considered). Although being longer, the execution time of single-level optimization (around 25 s) is still significantly lower than the charging sampling time of 15 minutes, thus making it appropriate for the case of considered fleet size.

Future work could be focused on the scalability of these charging methods for larger EV fleets. Also, as the considered idealized model input time profiles are typically not known exactly in advance in real applications, the future work could include sensitivity analyses related to predictions uncertainties.

## ACKNOWLEDGMENT

It is gratefully acknowledged that this work has been supported by the European Commission through Horizon 2020 Innovation action project OLGA (“hOListic Green Airport”) under Grant Agreement No. 101036871.

## APPENDIX

The expression for the grid power (10) which includes logical relations should be transferred to an equivalent form of inequality constraints, to be appropriate for MILP solvers [22]. Firstly, the minimum and maximum values of the function  $-P_{res}(k) + \sum_{i=1}^{N_v} P_{c,i}(k)$  are defined as:

$$m = \min \left( -P_{res}(k) + \sum_{i=1}^{N_v} P_{c,i}(k) \right) = -\max(P_{res}(k)) \quad (\text{A1a})$$

$$M = \max \left( -P_{res}(k) + \sum_{i=1}^{N_v} P_{c,i}(k) \right) = N_v P_{c,\max,i} \quad (\text{A1b})$$

which are derived based on the aggregate charging power limits:  $0 \leq \sum_{i=1}^{N_v} P_{c,i}(k) \leq N_v P_{c,\max,i}$ . By using the binary integer variable  $z(k)$  defined by Eq. (22), Eq. (10) can be rewritten as:

$$[z(k) = 0] \rightarrow [P_g(k) = 0], [z(k) = 1] \rightarrow \left[ P_g(k) = -P_{res}(k) + \sum_{i=1}^{N_v} P_{c,i}(k) \right]. \quad (\text{A2})$$

The expression (A3) can be written in the following form of inequalities [22]:

$$P_g(k) \leq Mz(k), \quad (\text{A3a})$$

$$P_g(k) \geq mz(k), \quad (\text{A3b})$$

$$P_g(k) \leq -P_{res}(k) + \sum_{i=1}^{N_v} P_{c,i}(k) - m(1 - z(k)), \quad (\text{A3c})$$

$$P_g(k) \geq -P_{res}(k) + \sum_{i=1}^{N_v} P_{c,i}(k) - M(1 - z(k)). \quad (\text{A3d})$$

It can be easily checked that the first two inequalities (A3a) and (A3b) forces the grid power to be zero ( $P_g(k) = 0$ ), when  $z(k) = 0$ , while two other inequalities (A3c) and (A3d) are relaxed

in that case (i.e., satisfied for any charging power request  $\sum_{i=1}^{N_v} P_{c,i}(k)$  and RES power  $P_{res}(k)$ ). On the other hand, when  $z(k) = 1$ , the first two constraints (A3a) and (A3b) are relaxed (according to the definitions in Eq. (A1)), while the remaining two forces the equality  $P_g(k) = -P_{res}(k) + \sum_{i=1}^{N_v} P_{c,i}(k)$  to be satisfied, as required by Eq. (A2).

Now, it remains to transfer the logical relation from Eq. (22) to the form of inequalities. This logical relation corresponds to the equivalence as:

$$\left[ -P_{res}(k) + \sum_{i=1}^{N_v} P_{c,i}(k) \geq 0 \right] \leftrightarrow [z(k) = 1]. \quad (\text{A4})$$

According to [22], the following equivalent inequalities can be established:

$$P_{res}(k) - \sum_{i=1}^{N_v} P_{c,i}(k) \leq M'(1 - z(k)), \quad (\text{A5a})$$

$$P_{res}(k) - \sum_{i=1}^{N_v} P_{c,i}(k) \geq \varepsilon + (m' - \varepsilon)z(k). \quad (\text{A5b})$$

where  $\varepsilon$  is a small positive constant (set to  $10^{-6}$ ), and  $m'$  and  $M'$  are defined as:

$$m' = \min \left( P_{res}(k) - \sum_{i=1}^{N_v} P_{c,i}(k) \right) = -N_v P_{c,\max,i}, \quad (\text{A6a})$$

$$M' = \max \left( P_{res}(k) - \sum_{i=1}^{N_v} P_{c,i}(k) \right) = \max(P_{res}). \quad (\text{A6b})$$

In conclusion, the set of inequalities (A3) and (A5) fully represents the starting logical expression (10).

## REFERENCES

1. Škugor, B. and Deur, J., Dynamic Programming-based Optimization of Charging an Electric Vehicle Fleet System Represented by an Aggregate Battery Model, *Energy*, Vol. 92, pp 456-466, 2015.
2. Škugor, B., Topić, J. and Deur, J., Quadratic Programming-based Electric Vehicle Charging Optimisation combining Charging Cost and Grid Power Peak Minimisation, *12<sup>th</sup> Conference on Sustainable Development of Energy, Water, and Environment Systems (SDEWES)*, Dubrovnik, Croatia, 2017.
3. Barman, P., Dutta, L., Bordoloi, S., et al., Renewable energy integration with electric vehicle technology: A review of the existing smart charging approaches, *Renewable and Sustainable Energy Reviews*, Vol. 183, 2023.
4. Škugor, B. and Deur, J., Analysis of Techno-economic Aspects of an Energy System Including Delivery Electric Vehicle Fleet and Renewable Energy Sources, *10<sup>th</sup> Conference of Sustainable Development of Energy, Water and Environment Systems (SDEWES)*, Dubrovnik, Croatia, 2015.
5. Dukpa, A. and Butrylo, B., MILP-Based Profit Maximization of Electric Vehicle Charging Station Based on Solar and EV Arrival Forecasts, *Energies*, Vol. 15, No. 15, 2022.
6. Mehrabi, A., et al., Decentralised Greedy-Based Algorithm for Smart Energy Management in Plug-in Electric Vehicle Energy Distribution Systems, *IEEE Access*, Vol. 8, 2020.
7. Lu, C., et al., Optimal fleet deployment for electric vehicle sharing systems with the consideration of demand uncertainty, *Computers & Operations Research*, Vol. 135, 2021.

8. Yao, Z., et. al., Smart charging and discharging of electric vehicles based on multi-objective robust optimization in smart cities, *Applied Energy*, Vol. 343, 2023.
9. Elmehdi, M., and Abdelilah, M., Genetic Algorithm for Optimal Charge Scheduling of Electric Vehicle Fleet, *2<sup>nd</sup> International Conference on Networking, Information Systems and Security*, Rabat, 2019.
10. Di Giorgio, A., Liberati, F. and Canale, S., Electric vehicles charging control in a smart grid: A model predictive control approach, *Control Engineering Practice*, Vol. 22, pp 147–162, 2014.
11. Diaz, C., Ruiz, F., and Patino, D., Smart Charge of an Electric Vehicles Station: A Model Predictive Control Approach, *IEEE Conference on Control and Applications*, Copenhagen, 2018.
12. Seddig, K., Jochem, P., and Fichtner, W., Integrating renewable energy sources by electric vehicle fleets under uncertainty, *Energy*, Vol. 141, pp 2145–2153, 2017.
13. Yang, Y. and Yeh, H., A Robust Model Predictive Control-Based Scheduling Approach for Electric Vehicle Charging with Photovoltaic Systems, *IEEE Systems journal*, Vol. 17, 2023.
14. Yamashita, D. Y., et al., Hierarchical Model Predictive Control to Coordinate a Vehicle-to-Grid System Coupled to Building Microgrids, *IEEE Transactions on Industry Applications*, Vol. 59, No. 1, pp 169–179, 2023.
15. Zheng, Y., Online Distributed MPC-Based Optimal Scheduling for EV Charging Stations in Distribution Systems, *IEEE Transactions on Industrial Informatics*, Vol. 15, No. 2, pp. 638–649, 2019.
16. Gromann, F., Raab, A. and Strunz, K., Optimal Charging Control of Electric Vehicle Fleets based on Demand Aggregation and User-Oriented Disaggregation Respecting Data Privacy, *IEEE Transactions on Transportation Electrification*, 2023.
17. Škugor, B. and Deur, J., Hierarchical Model Predictive Control-based Electric Vehicle Fleet Charging Management, *19<sup>th</sup> Conference on Sustainable Development of Energy, Water, and Environment Systems (SDEWES)*, Rome, 2024.
18. Škugor, B. and Deur, J., A Novel Model of Electric Vehicle Fleet Aggregate Battery for Energy Planning Studies, *Energy*, Vol. 92, pp 444-455, 2015.
19. Stadtler, H., Kilger, C. and Meyr, H., Supply Chain Management and Advanced Planning: Concepts, Models, Software and Case Studies, Springer, Berlin, 2015.
20. Lofberg, J., YALMIP: a toolbox for modeling and optimization in MATLAB, *IEEE International Conference on Robotics and Automation*, Taipei, 2004.
21. Škugor, B. and Deur, J., Delivery vehicle fleet data collection, analysis, and naturalistic driving cycle synthesis, *International Journal of Innovation and Sustainable Development*, Vol. 10, pp 19-39, 2016.
22. Bemporad, A. and Morari, M., Control of systems integrating logic, dynamics, and constraints, *Automatica*, Vol. 35, pp. 407-427, 1999.
23. Nocedal, J., and S. J. Wright: “Numerical Optimization”, *Springer Series in Operations Research and Financial Engineering*, 2nd edition, Springer, Berlin, 2006.